Robotica (2016) volume 34, pp. 2386–2399. © Cambridge University Press 2015
doi:10.1017/S026357471500003X

# Solving kinematics and stiffness of a novel n(2-UPS/PS+RPS) spatial hyper-redundant manipulator

Bo Hu†,‡,§,*, Yin Wang¶, Jingjing Yu‖ and Yi Lu†,‡

*†Parallel robot and mechatronic system laboratory of Hebei province, Yanshan University, Qinhuangdao, Hebei 066004, P. R. China*
*‡Key Laboratory of Advanced Forging & Stamping Technology and Science of Ministry of National Education, Yanshan University, Qinhuangdao, Hebei 066004, P. R. China*
*§State Key Laboratory of Robotics and System, Harbin Institute of Technology, Harbin, Heilongjiang, P. R. China*
*¶College of Mechanical Engineering, Hebei United University 063009,Tangshan, P. R. China*
*‖Department of Mechanics and Electronics, Heibei Normal University of Science & Technology, Qinhuangdao, P. R. China*

(Accepted January 06, 2015. First published online: February 11, 2015)

**SUMMARY**
A novel n(2-UPS/PS+RPS) spatial hyper-redundant manipulator (SHRM) formed by an optional number of 2-UPS/PS+RPS(2-universal joint-prismatic joint-spherical joint/prismatic joint-spherical joint+revolute joint-prismatic joint-spherical joint) parallel manipulators(PMs) connected in series is proposed and analyzed in this paper. First, the forward kinematics of the 2-UPS/PS+RPS PM is derived in close form. By extending this result to the whole SHRM, the forward kinematics model of the n(2-UPS/PS+RPS) SHRM is established. Second, the compact and elegant expressions for solving the forward velocity of the n(2-UPS/PS+RPS) SHRM are derived. Third, the statics and stiffness of the n(2-UPS/PS+RPS) SHRM are analyzed systematically by considering both active forces and constrained forces existed in each 2-UPS/PS+RPS PM. Finally, an analytically solved example is given for a 4(2-UPS/PS+RPS) SHRM formed by four 2-UPS/PS+RPS PMs. The analytical results are verified by CAD software.

KEYWORDS: Hyper-redundant manipulators; Kinematics; Statics; Stiffness.

## 1. Introduction

In recent years, SHRMs have attracted much attention in the field of robotics.[1,2] The SHRMs are formed by multi- PMs connected in series. This class of manipulators has large workspace, high manipulability, good obstacle avoidance ability and can be used as spatial truss, biomimetic snake, elephant's trunk, multi-tasking machining tools and so on.[3,4] In the aspect of SHRMs, Romdhane[5] proposed a hybrid SHRM formed by a pure translational and a pure rotational PMs. Lange *et al.*[6] studied the kinematics of an SHRM which is used as a swashplate mechanism of an unmanned aerial vehicle. Hu *et al.*[7,8] studied the kinematics of a class of SHRMs formed by a lower and an upper PM. Gallardo-Alvarado *et al.*[9–11] studied the kinematics of some SHRMs by using screw theory. Ibrahim and Khalil[12] established the inverse and direct dynamic models of hybrid robots by means of the recursive Newton–Euler algorithms. Liang and Ceccarelli[13,14] designed a waist–trunk system for a humanoid robot by using serial-parallel architectures. SHRMs have the advantages of both serial manipulators (SMs) and PMs from rigidity and workspace. However, the theory research such as kinematics, statics and stiffness for this class of manipulators include the difficulties of both SMs and PMs.

* Corresponding author. E-mail: hubo@ysu.edu.cn

Although some efforts have been spent on SHRMs due to their particular advantages, the research of this class of manipulators progressed at a slow pace. The deficiencies of the research of SHRMs mainly reflect in two aspects: First, the architectures of this class of manipulators are very limited. Second, the theoretical system for analyzing SHRMs has not been established due to their complex structures. In order to enrich the architectures and develop the theory of SHRMs, a novel n(2-UPS/PS+RPS) SHRM is proposed and analyzed in this paper. In the application field of the robot, some PMs with constrained legs[15–18] are frequently used to enhance the stiffness and motion precision. Motivated by this concept, a novel 2-UPS/PS+RPS PM is proposed and used as the individual module of the novel SHRM. Different from the existing PMs with constrained legs,[15–18] the proposed 2-UPS/PS+RPS PM has some particular advantages. In structure, this PM has three active legs and one PS constrained leg. The PS-type constrained leg can enhance the stiffness and provide high rotational capability for the PM. In addition, this PM has a high motion precision because most joints are spherical or prismatic joints. Due to the advantages of the single 2-UPS/PS+RPS PM, good performance of the n(2-UPS/PS+RPS) SHRM can be easily obtained. Compared with conventional SHRMs, the n(2-UPS/PS+RPS) SHRM has high stiffness and high motion ability and thus has some potential applications for the robot arms, the surgical manipulators, the machine tools, the tunnel borers, and the satellite surveillance platform.

Solving the kinematics, statics and stiffness is challenging work. The previous researches of SHRMs mainly focused on the kinematics based on the principle of motional superposition for the SHRMs formed by two PMs.[6–8] However, there are few efforts made towards SHRMs formed by an optional number of PMs.[9,10] In addition, most of the previous works adopted numerical approaches while the analytical solutions were seldom derived, which was not enough to guide the structure design of SHRMs.

For this reason, this paper focuses on establishing the kinematics, statics and stiffness model for a novel n(2-UPS/PS+RPS) SHRM. The established model provides the theory foundation for the application of this manipulator, and a feasible approach for solving kinematics and statics problems for other SHRMs.

The remainder of this paper is organized as follows. In Section 2, after a brief description of the novel n(2-UPS/PS+RPS) SHRM, the forward kinematics is derived in close form. Then the forward velocity is established based on the kinematic relation of each PM of the SHRM in Section 3. In Section 4, the statics and stiffness models are established. In Section 5, a numerical example concerned with the kinematics and stiffness of a 4(2-UPS/PS+RPS) SHRM is provided. Finally, some concluding remarks are given in Section 6.

## 2. Position Analysis of the n(2-UPS/PS+RPS) SHRM

### *2.1. Description of the n(2-UPS/PS+RPS) SHRM*

The n(2-UPS/PS+RPS) SHRM is formed by $n$ identical three degree of freedoms (DOFs) 2-UPS/PS+RPS PMs connected in sequence from bottom to top. Figure 1 shows a 4(2-UPS/PS+RPS) SHRM formed by four 2-UPS/PS+RPS PMs.

For the n(2-UPS/PS+RPS) SHRM, the $i$th 2-UPS/PS+RPS PM(see Fig. 2) has a upper platform $m_{i1}$, a lower platform $m_{io}$, three active driving legs $r_{ij}(i = 1, 2, ..., n; j = 1, 2, 3)$, and one passive limb $r_{oi}$. $m_{i0}$ is a regular triangle with three vertices$(A_{i1}, A_{i2}, A_{i3})$ and a center point $O_i$. $m_{i1}$ is a regular triangle with three vertices $(B_{i1}, B_{i2}, B_{i3})$ and a center point $o_i$. The first and the third active leg $r_{ij}(i = 1, 2, ..., n; j = 1, 3)$ connects $m_{io}$ with $m_{i1}$ by using a universal joint U at $A_{ij}$ on $m_{io}$, a prismatic joint P along $r_{ij}$, and a spherical joint S at $B_{ij}$ on $m_{i1}$. The second active leg $r_{i2}(i = 1, 2, ..., n)$ connects $m_{io}$ with $m_{i1}$ by using a revolute joint $R_i$ at $A_{i2}$ on $m_{io}$, a prismatic joint P along $r_{i2}$, and a spherical joint S at $B_{i2}$ on $m_{i1}$. $R_i$ is parallel with its opposite side $A_{i1}A_{i3}$. The passive leg $r_{oi}$ is perpendicular with $m_{io}$, and connects $m_{io}$ with $m_{i1}$ by using a prismatic joint P along $r_{oi}$, and a spherical joint S at $o_i$ on $m_{i1}$. All spherical joints in the SHRM are formed by three intersecting revolute joints. The upper platform of ($i$–1)th 2-UPS/PS+RPS PM and the lower platform of $i$th 2-UPS/PS+RPS PM are fixed connected with their centers kept coincidence and have an angle of $60 \times (-1)^i$ degrees between them.

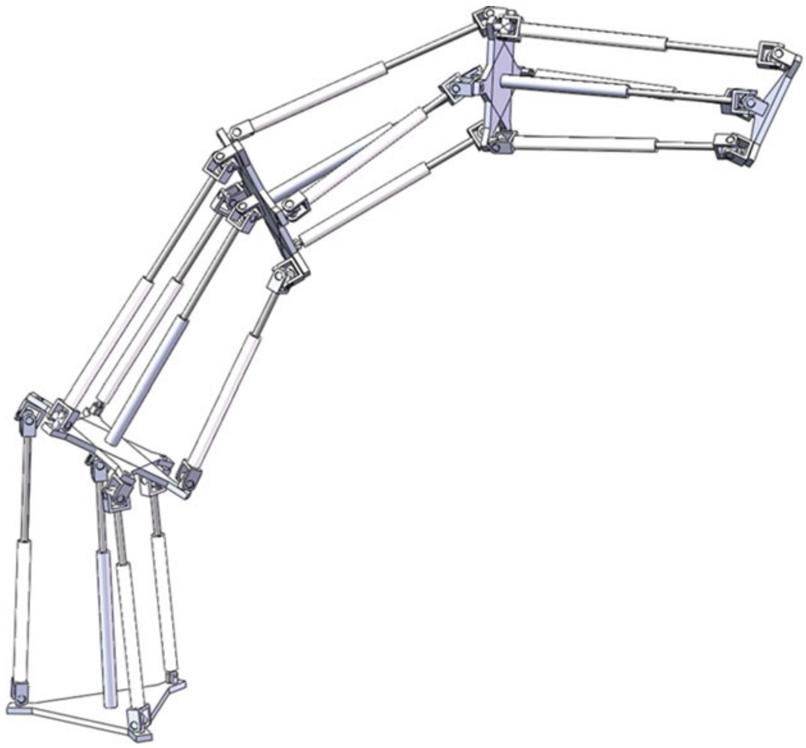

Fig. 1. CAD model of a 4(2-UPS/PS+RPS) SHRM.

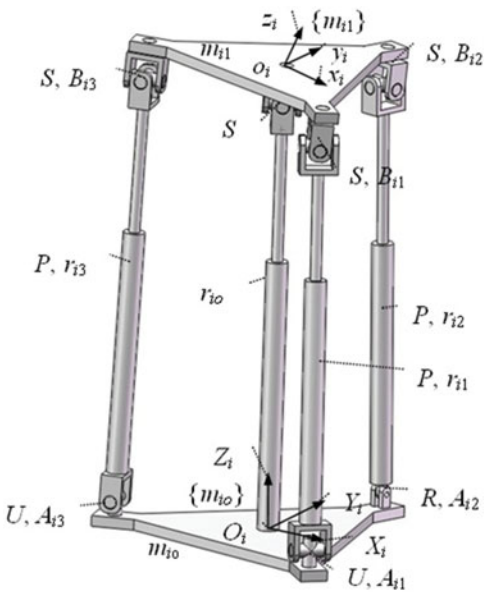


Fig. 2. CAD model of the 2-UPS/PS+RPS PM.

### *2.2. Forward position analysis of the 2-UPS/PS+RPS PM*

Let $\{m_{io}\}$ be the coordinate frame fixed on the center of $m_{io}$ with $O_i$ as its origin and $X_i$, $Y_i$, and $Z_i$ as its three coordinate axes. Let $\{m_{i1}\}$ be the coordinate frame at $m_{i1}$ with $o_i$ as its origin and $x_i$, $y_i$, and $z_i$ as its three coordinate axes. Some conditions ($X_i \perp A_{i1}A_{i2}$, $Y_i \| A_{i1}A_{i2}$, $Z_i \perp X_i$, $Z_i \perp Y_i$, $x_i \perp B_{i1}B_{i2}$, $y \| B_{i1}B_{i2}$, $z \perp x_i$, $z \perp y_i$) for the coordinate axes are satisfied.

The geometrical constraints in the *i*th 2-UPS/PS+RPS PM can be expressed as follows:

$$O_i o_i \perp X_i, O_i o_i \perp Y_i, A_{i2}B_{i2} \perp R_i, R_i || X_i. \tag{1}$$

https://doi.org/10.1017/S026357471500003X Published online by Cambridge University Press

The points $A_{ij}(i = 1, 2, ..., n; j = 1, 2, 3)$, $O_i$ and $o_i$ in $\{m_{io}\}$ can be expressed as follows:

$$^{m_{i0}}\boldsymbol{A}_{i1} = \frac{1}{2}\begin{bmatrix} qL_i \\ -L_i \\ 0 \end{bmatrix}, \ ^{m_{i0}}\boldsymbol{A}_{i2} = \begin{bmatrix} 0 \\ L_i \\ 0 \end{bmatrix}, \ ^{m_{i0}}\boldsymbol{A}_{i3} = -\frac{1}{2}\begin{bmatrix} qL_i \\ L_i \\ 0 \end{bmatrix},$$

$$^{m_{i0}}\boldsymbol{O}_i = \begin{bmatrix} 0 \\ 0 \\ 0 \end{bmatrix}, \ ^{m_{i0}}\boldsymbol{o}_i = \begin{bmatrix} X_{io} \\ Y_{io} \\ Z_{io} \end{bmatrix}, \ q = \sqrt{3}. \tag{2a}$$

Here, $L_i$ is the distance from $O_i$ to $A_{ij}$.

The points $B_{ij}(i = 1, 2, ..., n; j = 1, 2, 3)$ in $\{m_{i1}\}$ can be expressed as follows:

$$^{m_{i1}}\boldsymbol{B}_{i1} = \frac{1}{2}\begin{bmatrix} ql_i \\ -l_i \\ 0 \end{bmatrix}, \ ^{n_{i1}}\boldsymbol{B}_{i2} = \begin{bmatrix} 0 \\ l_i \\ 0 \end{bmatrix}, \ ^{n_{i1}}\boldsymbol{B}_{i3} = -\frac{1}{2}\begin{bmatrix} ql_i \\ l_i \\ 0 \end{bmatrix}. \tag{2b}$$

Here, $l_i$ is the distance from $o_i$ to $B_{ij}$.

The points $B_{ij}(i = 1, 2, ..., n; j = 1, 2, 3)$ in $\{m_{io}\}$ can be expressed as follows:

$$^{m_{i0}}\boldsymbol{B}_{ij} = {}^{m_{i0}}_{m_{i1}}\mathbf{R}\,^{m_{i1}}\boldsymbol{B}_{ij} + {}^{m_{i0}}\boldsymbol{o}_i \ \ (j = 1, 2, 3), \quad {}^{m_{i0}}_{m_{i1}}\mathbf{R} = \begin{bmatrix} x_{il} & y_{il} & z_{il} \\ x_{im} & y_{im} & z_{im} \\ x_{in} & y_{in} & z_{in} \end{bmatrix}. \tag{2c}$$

Where, $^{m_{i0}}\boldsymbol{o}_i$ is the position vector for the center of upper platform of $i$th PM relative to its lower platform. ${}^{m_{i0}}_{m_{i1}}\mathbf{R}$ is the rotational matrix from upper platform to lower platform for $i$th PM. $X_{io}$, $Y_{io}$, $Z_{io}$ are three components of position vector of $o_i$ in $\{m_{io}\}$.

Let ${}^{m_{i0}}_{m_{i1}}\mathbf{R}$ be formed by *ZXY* Euler rotations with $\alpha_i$, $\beta_i$, and $\lambda_i$ are three Euler angles about the corresponding axes, it leads to

$${}^{m_{i0}}_{m_{i1}}\mathbf{R} = \begin{bmatrix} c_{\alpha_i}c_{\lambda_i} - s_{\alpha_i}s_{\beta_i}s_{\lambda_i} & -s_{\alpha_i}c_{\beta_i} & c_{\alpha_i}s_{\lambda_i} + s_{\alpha_i}s_{\beta_i}c_{\lambda_i} \\ s_{\alpha_i}c_{\lambda_i} + c_{\alpha_i}s_{\beta_i}s_{\lambda_i} & c_{\alpha_i}c_{\beta_i} & s_{\alpha_i}s_{\lambda_i} - c_{\alpha_i}s_{\beta_i}c_{\lambda_i} \\ -c_{\beta_i}s_{\lambda_i} & s_{\beta_i} & c_{\beta_i}c_{\lambda_i} \end{bmatrix}. \tag{2d}$$

From Eq. (1), it leads to

$$\begin{aligned} &({}^{m_{i0}}\boldsymbol{o}_i - {}^{m_{i0}}\boldsymbol{O}_i) \cdot {}^{m_{i0}}\boldsymbol{X}_i = 0, \\ &({}^{m_{i0}}\boldsymbol{o}_i - {}^{m_{i0}}\boldsymbol{O}_i) \cdot {}^{m_{i0}}\boldsymbol{Y}_i = 0, \qquad {}^{m_{i0}}\boldsymbol{X}_i = \begin{bmatrix} 1 & 0 & 0 \end{bmatrix}^{\mathrm{T}}, \ {}^{m_{i0}}\boldsymbol{Y}_i = \begin{bmatrix} 0 & 1 & 0 \end{bmatrix}^{\mathrm{T}}. \\ &({}^{m_{i0}}\boldsymbol{B}_{i2} - {}^{m_{i0}}\boldsymbol{A}_{i2}) \cdot {}^{m_{i0}}\boldsymbol{X}_i = 0, \end{aligned} \tag{3}$$

The constrained equations for $i$th 2-UPS/PS+RPS PM can be derived from Eq. (3) as follows:

$$X_{io} = 0 \tag{4a}$$

$$X_{io} = -l_i y_{il} \tag{4b}$$

$$Y_{io} = 0. \tag{4c}$$

From Eqs. (2d), (4a), and (4b), it leads to

$$y_{il} = 0, \quad \alpha_i = 0, \quad {}^{m_{i0}}_{m_{i1}}\mathbf{R} = \begin{bmatrix} c_{\lambda_i} & 0 & s_{\lambda_i} \\ s_{\beta_i}s_{\lambda_i} & c_{\beta_i} & -s_{\beta_i}c_{\lambda_i} \\ -c_{\beta_i}s_{\lambda_i} & s_{\beta_i} & c_{\beta_i}c_{\lambda_i} \end{bmatrix}. \tag{4d}$$

https://doi.org/10.1017/S026357471500003X Published online by Cambridge University Press

Each extension of the driving limbs $r_i$ can be determined as follows:

$$r_{ij}^2 = |^{m_{i0}}\boldsymbol{B}_{ij} -^{m_{i0}} \boldsymbol{A}_{ij}|^2 \quad (i = 1, 2, \ldots, \ n; j = 1, 2, 3). \tag{5}$$

From Eqs. (4a)–(4d), and (5), the inverse kinematics of $i$th 2-UPS/PS+RPS PM can be derived as follows:

$$r_{i1}^2 = Z_{oi}^2 + L_i^2 + l_i^2 + ql_i x_{in} Z_{io} - ey_{in} Z_{oi} + L_i l_i (qx_{im} - 3x_{il} - y_{im})/2 \tag{6a}$$

$$r_2^2 = Z_{oi}^2 + L_i^2 + l_i^2 + 2l_i y_n Z_{io} - 2L_i l_i y_{im} \tag{6b}$$

$$r_{i3}^2 = Z_{oi}^2 + L_i^2 + l_i^2 - ql_i x_{in} Z_{io} - ey_{in} Z_{oi} - L_i l_i (qx_{im} + 3x_{il} + y_{im})/2. \tag{6c}$$

From Eqs. (6a)–(6c), and (4d), it leads to

$$r_{i3}^2 - r_{i1}^2 = 2ql_i Z_{oi} c_{\beta_i} s_{\lambda_i} - ql_i L_i s_{\beta_i} s_{\lambda_i} \tag{7a}$$

$$r_{i2}^2 = Z_{oi}^2 + L_i^2 + l_i^2 + 2l_i Z_{oi} s_{\beta_i} - 2L_i l_i c_{\beta_i} \tag{7b}$$

$$r_{i3}^2 + r_{i1}^2 - 2r_i 2^2 = -6l_i s_{\beta i} Z_{oi} + 3L_i l_i c_{\beta i} - 3l_i L_i c_{\lambda i}. \tag{7c}$$

From Eqs. (7a)–(7c), it leads to

$$s_{\lambda_i} = \frac{r_{i3}^2 - r_{i1}^2}{ql_i(2Z_{oi}c_{\beta_i} - L_i s_{\beta_i})}, \quad c_{\lambda_i} = \frac{2r_{i2}^2 - r_{i1}^2 - r_{i3}^2 - 6l_i Z_{oi} s_{\beta_i} + 3L_i l_i c_{\beta_i}}{3L_i l_i} \tag{8a}$$

$$s_{\lambda_i}^2 + c_{\lambda_i}^2 = \left[\frac{r_{i3}^2 - r_{i1}^2}{ql_i(2Z_{oi}c_{\beta_i} - L_i s_{\beta_i})}\right]^2 + \left[\frac{2r_{i2}^2 - r_{i1}^2 - r_{i3}^2 - 6l_i Z_{oi} s_{\beta_i} + 3L_i l_i c_{\beta_i}}{3L_i l_i}\right]^2 = 1. \tag{8b}$$

Let $t_i = tg_{(\beta_i/2)}$, it leads to

$$s_{\beta_i} = \frac{2t_i}{1 + t_i^2}, \quad c_{\beta_i} = \frac{1 - t_i^2}{1 + t_i^2}. \tag{9}$$

Substituting Eq. (9) into Eq. (7b) and multiplying the result by $(1 + t_i^2)$ to clear the denominators, leads to

$$\left(r_{i2}^2 - Z_{oi}^2 - L_i^2 - l_i^2 - 2L_i l_i\right) t_i^2 - 4l_i Z_{oi} t_i + r_{i2}^2 - Z_{oi}^2 - L_i^2 - l_i^2 + 2L_i l_i = 0. \tag{10}$$

Equation (10) can be expressed as following:

$$s_{i12} t_i^2 + s_{i11} t_i^2 + s_{i10} = 0. \tag{11}$$

Where, $s_{i12} = r_{i2}^2 - Z_{oi}^2 - L_i^2 - l_i^2 - 2L_i l_i, s_{i11} = -4l_i Z_{oi}, s_{i10} = r_{i2}^2 - Z_{oi}^2 - L_i^2 - l_i^2 + 2L_i l_i$.

Substituting Eq. (9) into Eq. (8b) and multiplying the result by $(1 + t_i^2)$ to clear the denominators, it leads to

$$\begin{aligned}
&\left(\frac{r_{i3}^2 - r_{i1}^2}{ql_i}\right)^2 \left(1 + t_i^2\right)^2 \\
&+ 4\left[\frac{\left(r_{i1}^2 + r_{i3}^2 - 2r_{i2}^2 + 3l_i L_i\right) t_i^2 + 12l_i Z_{oi} t_i^2 + r_{i1}^2 + r_{i3}^2 - 2r_{i2}^2 - 3l_i L_i}{3l_i L_i}\right]^2 \left(Z_{oi} t_i^2 + L_i t_i - Z_{oi}\right)^2 \\
&- 4\left(Z_{oi} t_i^2 + L_i t_i - Z_{oi}\right)^2 = 0.
\end{aligned} \tag{12}$$

Equation (12) can be expressed as following:

$$p_i \left(1 + t_i^2\right)^2 + \left(\sigma_{i2} t_i^2 + \sigma_{i1} t_i + \sigma_{i0}\right)^2 \left(\tau_{i2} t_i^2 + \tau_{i1} t_i + \tau_{i0}\right)^2 - \left(q_{i2} t_i^2 + q_{i1} t_i + q_{i0}\right)^2 = 0, \tag{13}$$

https://doi.org/10.1017/S026357471500003X Published online by Cambridge University Press

where

$$p_i = \left(\frac{r_{i3}^2 - r_{i1}^2}{ql_i}\right)^2, \sigma_{i2} = \frac{2\left(r_{i1}^2 + r_{i3}^2 - 2r_{i2}^2 + 3l_i L_i\right)}{3l_i L_i}, \sigma_{i1} = \frac{24Z_{oi}}{3L_i},$$

$$\sigma_{io} = \frac{2\left(r_{i1}^2 + r_{i3}^2 - 2r_{i2}^2 - 3l_i L_i\right)}{3l_i L_i}$$

$$\tau_{i2} = Z_{oi}, \tau_{i1} = L_i, \tau_{io} = -Z_{oi}, q_{i2} = 2Z_{oi}, q_{i1} = 2L_i, q_{io} = -2Z_{oi}.$$

The expanded form of Eq. (13) can be expressed as following:

$$s_{i28}t_i^8 + s_{i27}t_i^7 + s_{i26}t_i^6 + s_{i25}t_i^5 + s_{i24}t_i^4 + s_{i23}t_i^3 + s_{i22}t_i^2 + s_{i21}t_i + s_{i20} = 0, \tag{14}$$

where

$$\begin{aligned}
s_{i28} &= (\sigma_{i2}\tau_{i2})^2\\
s_{i27} &= 2\sigma_{i2}\tau_{i2}(\sigma_{i1}\tau_{i2} + \sigma_{i2}\tau_{i1})\\
s_{i26} &= (2\sigma_{io}\sigma_{i2} + \sigma_{i1}^2)\tau_{i2}^2 + 4\sigma_{i1}\sigma_{i2}\tau_{i1}\tau_{i2} + \sigma_{i2}^2(2\tau_{io}\tau_{i2} + \tau_{i1}^2)\\
s_{i25} &= 2\sigma_{io}\sigma_{i1}\tau_{i2}^2 + 2(2\sigma_{io}\sigma_{i2} + \sigma_{i1}^2)\tau_{i1}\tau_{i2} + 2\sigma_{i1}\sigma_{i2}(2\tau_{io}\tau_{i2} + \tau_{i1}^2) + 2\sigma_{i2}^2\tau_{io}\tau_{i1}\\
s_{i24} &= \sigma_{io}^2\tau_{i2}^2 + 4\sigma_{io}\sigma_{i1}\tau_{i1}\tau_{i2} + (2\sigma_{io}\sigma_{i2} + \sigma_{i1}^2)(2\tau_{io}\tau_{i2} + \tau_{i1}^2) + 4\sigma_{i1}\sigma_{i2}\tau_{io}\tau_{i1} + p_i - q_{i2}^2\\
s_{i23} &= -2q_{i1}q_{i2} + 2\sigma_{io}^2\tau_{i1}\tau_{i2} + 2\sigma_{io}\sigma_{i1}(2\tau_{io}\tau_{i2} + \tau_{i1}^2) + 2(2\sigma_{io}\sigma_{i2} + \tau_{i1}^2)\tau_{io}\tau_{i1} + 2\sigma_{i1}\sigma_{i2}\tau_{io}^2\\
s_{i22} &= -2q_{io}q_{i2} - q_{i1}^2 + 2p_i + \sigma_{io}^2(2\tau_{io}\tau_{i2} + \tau_{i1}^2) + 4\sigma_{io}\sigma_{i1}\tau_{io}\tau_{i1} + (2\sigma_{io}\sigma_{i2} + \sigma_{i1}^2)\tau_{io}^2\\
s_{i21} &= -2q_{io}q_{i1} + 2\sigma_{io}^2\tau_{io}\tau_{i1} + 2\sigma_{io}\sigma_{i1}\tau_{io}^2\\
s_{i20} &= p_i + \sigma_{io}^2\tau_{io}^2 - q_{io}^2.
\end{aligned}$$

Multiplying Eq. (11) by $t_i, t_i^2, t_i^3, t_i^4, t_i^5, t_i^6$, and $t_i^7$ respectively, seven equations can be obtained as following:

$$s_{i12}t_i^{j+2} + s_{i11}t_i^{j+1} + s_{i10}t_i^j = 0 \quad (j = 1 \ldots 7) \tag{15}$$

Multiplying Eq. (14) by $t_i$, leads to

$$s_{i28}t_i^9 + s_{i27}t_i^8 + s_{i26}t_i^7 + s_{i25}t_i^6 + s_{i24}t_i^5 + s_{i23}t_i^4 + s_{i22}t_i^3 + s_{i21}t_i^2 + s_{i20}t_i = 0. \tag{16}$$

Equations (11), (14), (15), and (16) form a system of ten linearly independent equations in ten variables $t^9$, $t^8$, $t^7$, $t^6$, $t^5$, $t^4$, $t^3$, $t^2$, $t$, and 1, which can be expressed in a matrix form as following

$$\mathbf{Q}_i \begin{bmatrix} t_i^9\\ t_i^8\\ t_i^7\\ t_i^6\\ t_i^5\\ t_i^4\\ t_i^3\\ t_i^2\\ t_i\\ 1 \end{bmatrix} = \begin{bmatrix}
s_{i28} & s_{i27} & s_{i26} & s_{i25} & s_{i24} & s_{i23} & s_{i22} & s_{i21} & s_{i20} & 0\\
0 & s_{i28} & s_{i27} & s_{i26} & s_{i25} & s_{i24} & s_{i23} & s_{i22} & s_{i21} & s_{i20}\\
0 & 0 & 0 & 0 & 0 & 0 & 0 & s_{i12} & s_{i11} & s_{i10}\\
0 & 0 & 0 & 0 & 0 & 0 & s_{i12} & s_{i11} & s_{i10} & 0\\
0 & 0 & 0 & 0 & 0 & s_{i12} & s_{i11} & s_{i10} & 0 & 0\\
0 & 0 & 0 & 0 & s_{i12} & s_{i11} & s_{i10} & 0 & 0 & 0\\
0 & 0 & 0 & s_{i12} & s_{i11} & s_{i10} & 0 & 0 & 0 & 0\\
0 & 0 & s_{i12} & s_{i11} & s_{i10} & 0 & 0 & 0 & 0 & 0\\
0 & s_{i12} & s_{i11} & s_{i10} & 0 & 0 & 0 & 0 & 0 & 0\\
s_{i12} & s_{i11} & s_{i10} & 0 & 0 & 0 & 0 & 0 & 0 & 0
\end{bmatrix} \begin{bmatrix} t_i^9\\ t_i^8\\ t_i^7\\ t_i^6\\ t_i^5\\ t_i^4\\ t_i^3\\ t_i^2\\ t_i\\ 1 \end{bmatrix} = 0 \tag{17}$$

https://doi.org/10.1017/S026357471500003X Published online by Cambridge University Press

To make sure Eq. (17) has nontrivial solutions, the following condition must be satisfied,

$$|\mathbf{Q}_i| = 0. \tag{18}$$

It is known that Eq. (18) is a nonlinear equation with regard to $Z_{io}$, thus $Z_{io}$ can be easily solved from Eq. (18). After $Z_{io}$ is solved, $\beta_i$ can be solved from Eq. (7b), and $\gamma_i$ can be solved by Eq. (7c) subsequently.

### 2.3. *Forward kinematics of n(2-UPS/PS+RPS) SHRM*

Since the platform $m_{i-1}$ and the $m_{io}$ are fixed connected with their centers kept coincidence and have an angle of $60 \times (-1)^i$ degrees between them, it leads to

$$^{m_{(i-1)1}}_{m_{i0}}\mathbf{R} = \begin{bmatrix} \cos[60^o \times (-1)^i] & -\sin[60^o \times (-1)^i] & 0 \\ \sin[60^o \times (-1)^i] & \cos[60^o \times (-1)^i] & 0 \\ 0 & 0 & 1 \end{bmatrix}, \tag{19}$$

where, $^{m_{(i-1)1}}_{m_{i0}}\mathbf{R}$ is the rotational matrix from $\{m_{io}\}$ to $\{m_{(i-1)1}\}$.

The center of the terminal platform $^{m_{10}}\boldsymbol{o}_n$ can be expressed as following:

$$^{m_{10}}\boldsymbol{o}_n = \sum_{i=1}^{n} {}^{m_{10}}_{m_{i0}}\mathbf{R}^{m_{i0}}\boldsymbol{o}_i,$$
$$^{m_{10}}_{m_{10}}\mathbf{R} = \mathbf{E}_{3\times3}, {}^{m_{10}}_{m_{i0}}\mathbf{R} = {}^{m_{10}}_{m_{10}}\mathbf{R}({}^{m_{10}}_{m_{11}}\mathbf{R}^{m_{11}}_{m_{20}}\mathbf{R}) \cdots ({}^{m_{(i-1)0}}_{m_{(i-1)1}}\mathbf{R}^{(i-1)1}_{m_{i0}}\mathbf{R}). \tag{20}$$

Where, $\mathbf{E}_{3\times3}$ is a 3×3 form identity matrix.

A composite rotational matrix $^{m_{10}}_{mn1}\mathbf{R}$ from $\{m_{n1}\}$ to $\{m_{10}\}$ can be expressed as following

$$^{m_{10}}_{m_{n1}}\mathbf{R} = {}^{m_{10}}_{m_{11}}\mathbf{R}({}^{m_{11}}_{m_{20}}\mathbf{R}^{m_{20}}_{m_{21}}\mathbf{R}) \cdots ({}^{m_{(i-1)1}}_{m_{i0}}\mathbf{R}^{m_{i0}}_{m_{i1}}\mathbf{R}) \cdots ({}^{m_{(n-1)1}}_{m_{n0}}\mathbf{R}^{m_{n0}}_{m_{n1}}R). \tag{21}$$

When the extensions of active legs $r_{ij}(i = 1, 2, ..., n; j = 1, 2, 3)$ are given, $Z_{io}$, $\beta_i$, and $\lambda_i$ can be solved, and $^{m_{10}}\boldsymbol{o}_n$ and $^{m_{10}}_{m_{i1}}\mathbf{R}$ can be solved from Eqs. (4d), (19), (20), and (21), subsequently.

## 3. Velocity of the n(2-UPS/PS+RPS) SHRM

Let $\boldsymbol{b} = [b_x b_y b_z]^{\mathrm{T}}$, $\boldsymbol{c} = [c_x c_y c_z]^{\mathrm{T}}$ be two arbitrary vectors, $S(b)$ be a skew-symmetric matrix. There must be

$$S(\boldsymbol{b}) = \begin{bmatrix} 0 & -b_z & b_y \\ b_z & 0 & -b_x \\ -b_y & b_x & 0 \end{bmatrix}, S(\boldsymbol{b}) = -S(\boldsymbol{b})^{\mathrm{T}}, \boldsymbol{b} \times \boldsymbol{c} = S(\boldsymbol{b})\boldsymbol{c}. \tag{22}$$

Let $^{m_{i0}}\boldsymbol{v}_{oi}$ and $^{m_{i0}}_{m_{i1}}\boldsymbol{\omega}$ be the linear velocity and angular velocity of upper platform relative to lower platform of the $i$th 2-UPS/PS+RPS PM, respectively. Let $v_{rij}(i = 1, 2, ..., n; j = 1, 2, 3)$ be the velocity of $r_{ij}$ and $\mathbf{J}_i$ be the inverse Jacobian matrix of $i$th 2-UPS/PS+RPS PM. The velocity of $r_{ij}$ can be as follows:[19]

$$\begin{bmatrix} v_{ri1} \\ v_{ri2} \\ v_{ri3} \end{bmatrix} = \begin{bmatrix} ^{m_{i0}}\boldsymbol{\delta}_{i1}^{\mathrm{T}} & (^{m_{i0}}\boldsymbol{e}_{i1} \times ^{m_{i0}}\boldsymbol{\delta}_{i1})^{\mathrm{T}} \\ ^{m_{i0}}\boldsymbol{\delta}_{i2}^{\mathrm{T}} & (^{m_{i0}}\boldsymbol{e}_{i2} \times ^{m_{i0}}\boldsymbol{\delta}_{i2})^{\mathrm{T}} \\ ^{m_{i0}}\boldsymbol{\delta}_{i3}^{\mathrm{T}} & (^{m_{i0}}\boldsymbol{e}_{i3} \times ^{m_{i0}}\boldsymbol{\delta}_{i3})^{\mathrm{T}} \end{bmatrix} \begin{bmatrix} ^{m_{i0}}\boldsymbol{v}_{oi} \\ ^{m_{i0}}\boldsymbol{\omega} \end{bmatrix}, {}^{m_{i0}}\boldsymbol{\delta}_{ij} = \frac{^{m_{i0}}\boldsymbol{B}_{ij} - ^{m_{i0}}\boldsymbol{A}_{ij}}{|^{m_{i0}}\boldsymbol{B}_{ij} - ^{m_{i0}}\boldsymbol{A}_{ij}|}, {}^{m_{i0}}\boldsymbol{e}_i = {}^{m_{i0}}\boldsymbol{B}_{ij} - {}^{m_{i0}}o. \tag{23}$$

For each 2-UPS/PS+RPS PM, there are constrained forces existed in the PS and RPS type legs. Based on the geometrical approach for determining constrained forces/torques,[19], two constrained forces $\boldsymbol{F}_{pi1}$ and $\boldsymbol{F}_{pi2}$ which pass through S joint and parallel with $m_{io}$ can be found in the PS leg. One constrained force $\boldsymbol{F}_{pi3}$ which passes through S joint and parallel with R joint can be found in the

https://doi.org/10.1017/S026357471500003X Published online by Cambridge University Press

RPS leg. From the geometrical constraints, the unit vectors $\boldsymbol{f}_{ij}$ of $\boldsymbol{F}_{pij}(i = 1, 2, ..., n; j = 1, 2, 3)$ are determined as follows:

$$^{m_{i0}}\boldsymbol{f}_{i1} = {}^{m_{i0}}\boldsymbol{f}_{i3} = {}^{m_{i0}}\boldsymbol{X}_i = \begin{bmatrix} 1 & 0 & 0 \end{bmatrix}^{\mathrm{T}}, \boldsymbol{f}_{i2} = {}^{m_{i0}}\boldsymbol{Y}_i = \begin{bmatrix} 0 & 1 & 0 \end{bmatrix}^{\mathrm{T}}. \tag{24}$$

In each 2-UPS/PS+RPS PM, as the constrained forces do no work to $m_{i1}$, it leads to

$$\begin{gathered} F_{pij}^{m_{i0}}\boldsymbol{f}_{ij} \cdot {}^{m_{i0}}\boldsymbol{v} + \left({}^{m_{i0}}\boldsymbol{d}_{ij} \times F_{pij}^{m_{i0}}\boldsymbol{f}_{ij}\right) \cdot {}^{m_{i0}}\boldsymbol{\omega} = 0, \\ \begin{bmatrix} {}^{m_{i0}}\boldsymbol{f}_{ij}^{\mathrm{T}} & \left({}^{m_{i0}}\boldsymbol{d}_{ij} \times {}^{m_{i0}}\boldsymbol{f}_{ij}\right)^{\mathrm{T}} \end{bmatrix} \begin{bmatrix} {}^{m_{i0}}\boldsymbol{v}_{oi} \\ {}^{m_{i0}}\boldsymbol{\omega} \end{bmatrix} = 0, \\ {}^{m_{i0}}\boldsymbol{d}_{i1} = {}^{m_{i0}}\boldsymbol{d}_{i2} = -{}^{m_{i0}}\boldsymbol{o}_i, {}^{m_{i0}}\boldsymbol{d}_{i3} = {}^{m_{i0}}\boldsymbol{B}_{ij} - {}^{m_{i0}}\boldsymbol{o}_i \end{gathered} \tag{25}$$

The inverse/forward velocities can be derived from Eqs. (23) and (25) as follows

$$\boldsymbol{v}_{ri} = \mathbf{J}_i \begin{bmatrix} {}^{m_{i0}}\boldsymbol{v}_{oi} \\ {}^{m_{i0}}\boldsymbol{\omega} \end{bmatrix}, \begin{bmatrix} {}^{m_{i0}}\boldsymbol{v}_{oi} \\ {}^{m_{i0}}\boldsymbol{\omega} \end{bmatrix} = \mathbf{J}_i^{-1}\boldsymbol{v}_{ri}, \boldsymbol{v}_{ri} = \begin{bmatrix} v_{ri1} \\ v_{ri2} \\ v_{ri3} \\ 0 \\ 0 \\ 0 \end{bmatrix}, \mathbf{J}_i = \begin{bmatrix} {}^{m_{i0}}\boldsymbol{\delta}_{i1}^{\mathrm{T}} & \left({}^{m_{i0}}\boldsymbol{e}_{i1} \times {}^{m_{i0}}\boldsymbol{\delta}_{i1}\right)^{\mathrm{T}} \\ {}^{m_{i0}}\boldsymbol{\delta}_{i2}^{\mathrm{T}} & \left({}^{m_{i0}}\boldsymbol{e}_{i2} \times {}^{m_{i0}}\boldsymbol{\delta}_{i2}\right)^{\mathrm{T}} \\ {}^{m_{i0}}\boldsymbol{\delta}_{i3}^{\mathrm{T}} & \left({}^{m_{i0}}\boldsymbol{e}_{i3} \times {}^{m_{i0}}\boldsymbol{\delta}_{i3}\right)^{\mathrm{T}} \\ {}^{m_{i0}}\boldsymbol{f}_{i1}^{\mathrm{T}} & \left({}^{m_{i0}}\boldsymbol{d}_{i1} \times {}^{m_{i0}}\boldsymbol{f}_{i1}\right)^{\mathrm{T}} \\ {}^{m_{i0}}\boldsymbol{f}_{i2}^{\mathrm{T}} & \left({}^{m_{i0}}\boldsymbol{d}_{i2} \times {}^{m_{i0}}\boldsymbol{f}_{i2}\right)^{\mathrm{T}} \\ {}^{m_{i0}}\boldsymbol{f}_{i3}^{\mathrm{T}} & \left({}^{m_{i0}}\boldsymbol{d}_{i3} \times {}^{m_{i0}}\boldsymbol{f}_{i3}\right)^{\mathrm{T}} \end{bmatrix}. \tag{26}$$

From Eq. (26), ${}^{m_{i0}}\boldsymbol{v}_{oi}$ and ${}^{m_{i0}}\boldsymbol{\omega}$ can be solved when $v_{rij}(i = 1, 2, ..., n; j = 1, 2, 3)$ are given.

For the n(2-UPS/PS+RPS) SHRM, let ${}^{m_{10}}_{mn1}\boldsymbol{\omega}$ and ${}^{m_{10}}\boldsymbol{v}_{\mathrm{on}}$ be the angular velocity and linear velocity of terminal platform $m_{n1}$ relative to $\{m_{10}\}$.${}^{m_{10}}_{mn1}\boldsymbol{\omega}$ can be derived as following

$$^{m_{10}}_{m_{n1}}\boldsymbol{\omega} = \sum_{i=1}^{n} {}^{m_{10}}_{m_{i0}}\mathbf{R}^{m_{i0}}_{m_{i1}}\boldsymbol{\omega}, {}^{m_{10}}_{m_{i1}}\mathbf{R} = {}^{m_{10}}_{m_{i0}}\mathbf{R}^{m_{i0}}_{m_{i1}}\mathbf{R}, {}^{m_{10}}_{m_{i1}}\mathbf{R} = {}^{m_{10}}_{m_{11}}\mathbf{R}\left({}^{m_{11}}_{m_{20}}\mathbf{R}^{m_{20}}_{m_{21}}\mathbf{R}\right) \cdots \left({}^{m_{(i-1)1}}_{m_{i0}}\mathbf{R}^{m_{i0}}_{m_{i1}}\mathbf{R}\right). \tag{27}$$

By differentiating both sides of the first item of Eq. (20), ${}^{m_{10}}\boldsymbol{v}_{\mathrm{on}}$ can be derived as following:

$$^{m_{10}}\boldsymbol{v}_{\mathrm{on}} = \sum_{i=1}^{n} \left[{}^{m_{10}}_{m_{i0}}\mathbf{R}^{m_{i0}}\boldsymbol{v}_{oi} + \left({}^{m_{10}}_{m_{i0}}\boldsymbol{\omega} \times {}^{m_{10}}_{m_{i0}}\mathbf{R}\right){}^{m_{i0}}\boldsymbol{o}_i\right]. \tag{28}$$

From Eq. (28), it leads to

$$^{m_{10}}\boldsymbol{v}_{\mathrm{on}} = \sum_{i=1}^{n} {}^{m_{10}}_{m_{i0}}\mathbf{R}^{m_{i0}}\boldsymbol{v}_{oi} - \sum_{i=1}^{n-1}\left\{\left[\sum_{j=i}^{n-1} S\left({}^{m_{10}}_{m_{(j+1)0}}\mathbf{R}^{m_{(j+1)0}}\boldsymbol{o}_{j+1}\right)\right]{}^{m_{10}}_{m_{i0}}\mathbf{R}^{m_{i0}}_{m_{i1}}\boldsymbol{\omega}\right\}(n \geq 2). \tag{29}$$

By combing Eq. (27) with (29), it leads to

$$\begin{gathered} \begin{bmatrix} {}^{m_{10}}\boldsymbol{v}_{\mathrm{on}} \\ {}^{m_{10}}_{m_{n1}}\boldsymbol{\omega} \end{bmatrix} = \sum_{i=1}^{n} \mathbf{J}_{Ri} \begin{bmatrix} {}^{m_{i0}}\boldsymbol{v}_{oi} \\ {}^{m_{i0}}_{m_{i1}}\boldsymbol{\omega} \end{bmatrix} (n \geq 2) \\ \mathbf{J}_{Ri} = \begin{bmatrix} {}^{m_{10}}_{m_{i0}}\mathbf{R} & -\left[\sum_{j=i}^{n-1} S\left({}^{m_{10}}_{m_{(j+1)0}}\mathbf{R}^{m_{(j+1)0}}\boldsymbol{o}_{j+1}\right)\right]{}^{m_{10}}_{m_{i0}}\mathbf{R} \\ \mathbf{0}_{3\times 3} & {}^{m_{10}}_{m_{i0}}\mathbf{R} \end{bmatrix} (i < n), \\ \mathbf{J}_{Rn} = \begin{bmatrix} {}^{m_{10}}_{m_{i0}}\mathbf{R} & 0_{3\times 3} \\ \mathbf{0}_{3\times 3} & {}^{m_{10}}_{m_{i0}}\mathbf{R} \end{bmatrix} (i = n). \end{gathered} \tag{30}$$

https://doi.org/10.1017/S026357471500003X Published online by Cambridge University Press

From Eq. (30), the velocity of the n(2-UPS/PS+RPS) SHRM formed by an optional number of 2-UPS/PS+RPS PMs can be solved.

## 4. Statics and Stiffness of The n(2SPS+RPS+PS) SHRM

Let $F$ and $T$ be the external force and torque applied on the terminal platform $m_{n1}$. Let $F_{rij}(i = 1, 2, ..., n; j = 1, 2, 3)$ be the active forces and $F_{pij}(i = 1, 2, ..., n; j = 1, 2, 3)$ be the constrained forces of the $i$th 2-UPS/PS+RPS PM. For the statics and stiffness analysis, suppose the rigid platform $m_{io}$ and $m_{i1}$ is elastically suspended by the elastic active legs with equal cross section. By applying the principle of virtue work and combining with Eq. (30), it leads to

$$\boldsymbol{F}_{s1}^{\mathrm{T}}\boldsymbol{v}_{r1} + \boldsymbol{F}_{s2}^{\mathrm{T}}\boldsymbol{v}_{r2} + \cdots + \boldsymbol{F}_{sn}^{\mathrm{T}}\boldsymbol{v}_{rn} = -\begin{bmatrix} {}^{m_{10}}\boldsymbol{F} \\ {}^{m_{10}}\boldsymbol{T} \end{bmatrix}^{\mathrm{T}} \begin{bmatrix} {}^{m_{10}}\boldsymbol{v}_{\mathrm{on}} \\ {}^{m_{10}}_{m_{n1}}\boldsymbol{\omega} \end{bmatrix} = -\begin{bmatrix} {}^{m_{10}}\boldsymbol{F} \\ {}^{m_{10}}\boldsymbol{T} \end{bmatrix}^{\mathrm{T}} \sum_{i=1}^{n} \mathbf{J}_{Ri} \begin{bmatrix} {}^{m_{i0}}\boldsymbol{v}_{oi} \\ {}^{m_{i0}}_{m_{i1}}\boldsymbol{\omega} \end{bmatrix}$$

$$= -\begin{bmatrix} {}^{m_{10}}\boldsymbol{F} \\ {}^{m_{10}}\boldsymbol{T} \end{bmatrix}^{\mathrm{T}} \sum_{i=1}^{n} \mathbf{J}_{Ri}\mathbf{J}_i^{-1}\boldsymbol{v}_{ri}$$

$$\boldsymbol{F}_{si} = \begin{bmatrix} F_{ri1} & F_{ri2} & F_{ri3} & F_{pi1} & F_{pi2} & F_{pi3} \end{bmatrix}^{\mathrm{T}}, \boldsymbol{v}_{ri} = \begin{bmatrix} v_{ri1} & v_{ri2} & v_{ri3} & 0 & 0 & 0 \end{bmatrix}^{\mathrm{T}}. \quad (31)$$

where, $\boldsymbol{F}_{si}(i = 1, 2, ..., n)$ is a six dimensional vector formed by the active and constrained forces of the $i$th 2-UPS/PS+RPS PM, ${}^{m_{10}}\boldsymbol{F}$ and ${}^{m_{10}}\boldsymbol{T}$ are the external force and torque applied on terminal platform $\{m_{n1}\}$ relative to base $\{m_{10}\}$.

From Eq. (31), it leads to

$$\begin{bmatrix} \boldsymbol{F}_{s1}^{\mathrm{T}} & \cdots & \boldsymbol{F}_{sn}^{\mathrm{T}} \end{bmatrix} \begin{bmatrix} \boldsymbol{v}_{r1} \\ \vdots \\ \boldsymbol{v}_{rn} \end{bmatrix} = -\begin{bmatrix} {}^{m_{10}}\boldsymbol{F} \\ {}^{m_{10}}\boldsymbol{T} \end{bmatrix}^{\mathrm{T}} \begin{bmatrix} \mathbf{J}_{R1}\mathbf{J}_1^{-1} & \cdots & \mathbf{J}_{Rn}\mathbf{J}_n^{-1} \end{bmatrix} \begin{bmatrix} \boldsymbol{v}_{r1} \\ \vdots \\ \boldsymbol{v}_{rn} \end{bmatrix}. \quad (32a)$$

From Eq. (32a), it leads to

$$\boldsymbol{F}_{si} = -(\mathbf{J}_{Ri}\mathbf{J}_i^{-1})^{\mathrm{T}} \begin{bmatrix} {}^{m_{10}}\boldsymbol{F} \\ {}^{m_{10}}\boldsymbol{T} \end{bmatrix}. \quad (32b)$$

From Eq. (32b), $F_{rij}$ and $F_{pij}(i = 1, 2, ..., n; j = 1, 2, 3)$ can be solved when ${}^{m_{10}}\boldsymbol{F}$ and ${}^{m_{10}}\boldsymbol{T}$ are given.

Let $\delta r_{ij}(i = 1, 2, ..., n; j = 1, 2, 3)$ denotes the flexibility deformations along $r_{ij}(i = 1, 2, 3)$ due to the active force $F_{rij}$,, it leads to

$$F_{rij} = k_{rij}\delta r_{ij}, \quad k_{rij} = \frac{ES_{ij}}{r_{ij}}, \quad (33a)$$

where $E$ is the modular of elasticity and $S_{ij}$ denotes the $j$th leg's cross section of the $i$th 2-UPS/PS+RPS PM.

Let $\delta d_{ij}$ denotes the bending deformation of $r_{ij}(i = 1, 2, ..., n; j = 1, 2, 3)$ due to the constrained forces $F_{pij}$. The direction of this deformation can be considered along $F_{pi}$.

The relation between $F_{pij}$ and $\delta d_i$ can be expressed as follows:

$$F_{pij} = u_{ij}\delta d_{ij}(1{,}2{,}3), \quad u_{ij} = \frac{3EI}{r_{ij}^3} \quad (33b)$$

where, $I$ is the moment of inertia.

https://doi.org/10.1017/S026357471500003X Published online by Cambridge University Press

Table I. The dimension and kinematic parameters of *i*th PM.

| | $L_i$(m) | $l_i$(m) | $r_{i1}(m)$ | $r_{i2}(m)$ | $r_{i3}(m)$ | $v_{ri1}(m/s)$ | $v_{ri2}(m/s)$ | $v_{ri3}(m/s)$ |
|---|---|---|---|---|---|---|---|---|
| PM 1 | 1.10 | 0.9 | 1.10 | 1.30 | 1.40 | 0.5 | 0.5 | 0.5 |
| PM 2 | 1.00 | 0.8 | 1.00 | 1.20 | 1.30 | 0.5 | 0.5 | 0.5 |
| PM 3 | 0.90 | 0.7 | 0.90 | 1.10 | 1.20 | 0.5 | 0.5 | 0.5 |
| PM 4 | 0.80 | 0.6 | 0.80 | 1.00 | 1.10 | 0.5 | 0.5 | 0.5 |

From Eqs. (33a) and (33b), it leads to

$$\boldsymbol{F}_{si} = \mathbf{K}_{pi}\begin{bmatrix}\delta\boldsymbol{r}_i\\ \delta\boldsymbol{d}_i\end{bmatrix}, \delta\boldsymbol{r}_i = \begin{bmatrix}\delta r_{i1}\\ \delta r_{i2}\\ \delta r_{i3}\end{bmatrix}, \delta\boldsymbol{d}_i = \begin{bmatrix}\delta d_{i1}\\ \delta d_{i2}\\ \delta d_{i3}\end{bmatrix}, \mathbf{K}_{pi} = \begin{bmatrix} k_{ri1} & 0 & 0 & 0 & 0 & 0\\ 0 & k_{ri2} & 0 & 0 & 0 & 0\\ 0 & 0 & k_{ri3} & 0 & 0 & 0\\ 0 & 0 & 0 & u_{i1} & 0 & 0\\ 0 & 0 & 0 & 0 & u_{i2} & 0\\ 0 & 0 & 0 & 0 & 0 & u_i3 \end{bmatrix}. \tag{34}$$

Based on the principle of virtual work and combing Eq. (32b), it leads to

$$\boldsymbol{F}_{s1}^{\mathrm{T}}\begin{bmatrix}\delta\boldsymbol{r}_1\\ \delta\boldsymbol{d}_1\end{bmatrix} + \boldsymbol{F}_{s2}^{\mathrm{T}}\begin{bmatrix}\delta\boldsymbol{r}_2\\ \delta\boldsymbol{d}_2\end{bmatrix} + \cdots + \boldsymbol{F}_{sn}^{\mathrm{T}}\begin{bmatrix}\delta\boldsymbol{r}_n\\ \delta\boldsymbol{d}_n\end{bmatrix} = -\begin{bmatrix}{}^{m_{10}}\boldsymbol{F}\\ {}^{m_{10}}\boldsymbol{T}\end{bmatrix}^{\mathrm{T}}$$

$$\delta\boldsymbol{\rho} = -\begin{bmatrix}{}^{m_{10}}\boldsymbol{F}\\ {}^{m_{10}}\boldsymbol{T}\end{bmatrix}^{\mathrm{T}} \sum_{i=1}^{n}\left(\mathbf{J}_{Ri}\mathbf{J}_i^{-1}\right)\begin{bmatrix}\delta\boldsymbol{r}_i\\ \delta\boldsymbol{d}_i\end{bmatrix}, \tag{35}$$

where, $\delta\boldsymbol{\rho}$ is the deformation of $m_{n1}$. From Eq. (35), it leads to

$$\delta\boldsymbol{\rho} = \sum_{i=1}^{n}(J_{Ri}J_i^{-1})\begin{bmatrix}\delta\boldsymbol{r}_i\\ \delta\boldsymbol{d}_i\end{bmatrix}. \tag{36}$$

From Eqs. (32b), (34) and (36), it leads to

$$\begin{bmatrix}{}^{m_{10}}\boldsymbol{F}\\ {}^{m_{10}}\boldsymbol{T}\end{bmatrix} = \mathbf{K}\delta\boldsymbol{\rho}, \mathbf{K} = -\left[\sum_{i=1}^{n}(\mathbf{J}_{Ri}\mathbf{J}_i^{-1})\mathbf{K}_{pi}^{\mathrm{T}}(\mathbf{J}_{Ri}\mathbf{J}_i^{-1})^{\mathrm{T}}\right]^{-1}. \tag{37}$$

Here, **K** is a 6× 6 stiffness matrix of the n(2-UPS/PS+RPS) SHRM.

## 5. Analytically Solved Example

In this section, the computation of 4(2-UPS/PS+RPS) SHRM is performed applying the established kinematics, statics and stiffness model. The dimension and kinematic parameters of the each 2-UPS/PS+RPS PM are chosen as follows.

Based on the dimension and kinematic parameters of each 2-UPS/PS+RPS PM listed in Table I, $Z_{io}$ of the *i*th ($i = 1, 2, 3, 4$) 2-UPS/PS+RPS PM are solved as follows.

The results show that each 2-UPS/PS+RPS PM has 24 solutions, which leads to the 4(2-UPS/PS+RPS) SHRM has $24^4 = 331{,}776$ solutions.

In order to determine the acceptable analytic solutions from multi-solutions, the simulation mechanisms of the 2-UPS/PS+RPS PM and the 4(2-UPS/PS+RPS) SHRM are created[20] using CAD software. When given the dimension parameters according to Table I for simulation mechanisms in CAD software, the forward kinematics of single 2-UPS/PS+RPS PM can be solved. From the

https://doi.org/10.1017/S026357471500003X Published online by Cambridge University Press

Table II. The 24 solutions of $Z_{1o}$, $Z_{2o}$, $Z_{3o}$, $Z_{4o}$.

| | | | | |
|---|---|---|---|---|
| $Z_{1o}$ | 1.0218 | −1.0218, | 1.2642, | −1.2642, |
| | 1.6275+0.1104i | −1.6275–0.1104i | 0.8514–0.09746i | −0.8514+0.097i |
| | 0.7414–0.0371i | −0.7414+0.0371i | −0.14038i | 0.14038i |
| | −0.21182i | 0.21182i | −0.28624i | 0.28624i |
| | −0.38351i | 0.38351i | 0.7414+0.0371i | −0.7414+0.0371i |
| | 0.8514+0.097i | −0.8514–0.097i | 1.6275+0.1104i | −1.6275–0.1104i |
| $Z_{2o}$ | 0.9610 | −0.9610 | 1.1638 | −1.1638 |
| | 1.4957+0.1112i | −1.4957–0.1112i | 0.8116–0.0073i | −0.8116+0.0073i |
| | 0.6986–0.3546i | −0.6986+0.3546i | −0.12686i | 0.12686i |
| | −0.18626i | 0.18626i | −0.27691i | 0.27691i |
| | −0.3426i | 0.3426i | 0.6986+0.0355i | −0.6986–0.0355i |
| | 0.8116+0.0073i | −0.8116–0.0073i | 1.4957+0.1112i | −1.4957–0.1112i |
| $Z_{3o}$ | 0.89936 | −0.89936 | 1.0633 | −1.0633 |
| | 0.7703–0.5142i | −0.7703+0.5142i | 1.3634–0.0107i | −1.3634+0.0107i |
| | 0.6564–0.0329i | −0.6564+0.0329i | −0.11154i | 0.11154i |
| | −0.16192i | 0.16192i | −0.26427i | 0.26427i |
| | −0.3014i | 0.3014i | 0.65636+0.0329i | −0.65636–0.0329i |
| | 1.3634+0.0107i | −1.3634–0.0107i | 0.7703+0.005i | −0.7703–0.005i |
| $Z_{4o}$ | 0.83682 | −0.83682 | 0.96242 | −0.96242 |
| | 0.7269–0.0336i | 0.7269–0.0336i | 1.2302–0.0992i | −1.2302+0.0992i |
| | 0.6149–0.2951i | −0.6149+0.2951i | −0.094486i | 0.094486i |
| | −0.13905i | 0.13905i | −0.24818i | 0.24818i |
| | −0.25988i | 0.25988i | 0.61498+0.0295i | −0.61498–0.0295i |
| | 1.2302+0.0099i | −1.2302–0.0099i | 0.72696+0.0034i | −0.72696–0.0034i |

simulation result, it can be seen that the simulation solution is in excellent agreement with the first solution obtained from the analytic method that are marked in Table II. By applying this solution to the 4(2-UPS/PS+RPS) SHRM, the position and velocity of the terminal platform are solved as follows:

$$^{m_{10}}\boldsymbol{o}_4 = \begin{bmatrix} 1.7949 & 0.3221 & 3.6872 \end{bmatrix}^{\mathrm{T}} \mathrm{m}$$

$$^{m_{10}}\boldsymbol{v}_{o4} = [0.8663 \quad 0.1639 \quad 1.6290]^{\mathrm{T}}\, \mathrm{m/s}$$

$$^{m_{10}}_{m_{41}}\boldsymbol{\omega} = \begin{bmatrix} -0.0376^{\circ} - 0.6594^{\circ} - 0.0202^{\circ} \end{bmatrix}^{\mathrm{T}} /\mathrm{s}.$$

Set $E = 2.11 \times 10^{11}$Pa, $EI = 26502\mathrm{N}\cdot\mathrm{m}^2$, $S_i = 0.0013\mathrm{m}^2$, $G = 80 \times 10^9$Pa, $I_p = 2.5120 \times 10^{-7}\mathrm{m}^4$. When the workloads applied at $o_4$ is given as $^{n_0}\boldsymbol{F}_o = [-30 - 30 - 50]^{\mathrm{T}} N$, $^{n_0}\boldsymbol{T}_o = [000]^{\mathrm{T}} N \cdot m$, the active forces and constrained forces in $r_{ij}$ and $r_{oi}$ can be solved as following (see Table III).

The flexibility and bending deformations of $r_{ij}$ and $r_{oi}$ can be solved as following (see Table IV.). The deformation of the terminal platform of 4(2-UPS/PS+RPS) SHRM is solved as following:

$$\delta\boldsymbol{\rho} = (-0.0038\ \mathrm{mm}\ 0.0259\ \mathrm{mm}\ 0.0025\ \mathrm{mm}\ 0.0033\ \mathrm{rad} - 0.0008\ \mathrm{rad}\ 0.0169\ \mathrm{rad})^T.$$

The stiffness matrix of 4(2-UPS/PS+RPS) SHRM is derived as following:

$$\mathbf{K} = 10^4 \begin{bmatrix} -4.7480 & -0.5204 & -4.5221 & -0.1795 & -1.4845 & 0.1955 \\ -0.5204 & -0.9911 & -0.4360 & -0.6030 & -1.0947 & 1.3556 \\ -4.5221 & -0.4360 & -9.3479 & -0.4876 & -5.2015 & 0.5989 \\ -0.1795 & -0.6030 & -0.4876 & -1.4247 & 1.2470 & 1.2917 \\ -1.4845 & -1.0947 & -5.2015 & 1.2470 & -17.582 & 1.0546 \\ 0.1955 & 1.3556 & 0.5989 & 1.2917 & 1.0546 & -2.3239 \end{bmatrix}.$$

To verify the analytical result, a finite element (FE) model for 4(2-UPS/PS+RPS) SHRM is established in FE software according to the dimensional and material parameters used in the analytical

https://doi.org/10.1017/S026357471500003X Published online by Cambridge University Press

Table III. Active forces and constrained forces in $r_{ij}$ and $r_{oi}$.

| | $F_{ri1}(N)$ | $F_{ri2}(N)$ | $F_{ri3}(N)$ | $F_{pi1}(N)$ | $F_{pi2}(N)$ | $F_{pi3}(N)$ |
|---|---|---|---|---|---|---|
| PM 1 | 71.6545 | −57.0875 | 35.6488 | 71.6545 | 118.0135 | −84.9927 |
| PM 2 | 29.8348 | −38.1541 | 63.6954 | 83.5186 | 2.0864 | −50.1357 |
| PM 3 | 85.5020 | −11.7935 | −9.5606 | 21.7679 | 10.6394 | −16.0225 |
| PM 4 | 19.7716 | 17.8153 | 17.3832 | 3.5481 | 35.7170 | 0.4395 |

Table IV. Deformations in $r_{ij}$ and $r_{oi}$.

| | $\delta r_{i1}(10^{-7}\text{m})$ | $\delta r_{i2}(10^{-7}\text{m})$ | $\delta r_{i3}(10^{-7}\text{m})$ | $\delta d_{i1}(10^{-5}\text{m})$ | $\delta d_{i2}(10^{-3}\text{m})$ | $\delta d_{i3}(10^{-3}\text{m})$ |
|---|---|---|---|---|---|---|
| PM 1 | 2.9725 | −2.8004 | 1.8826 | 29.9764 | 6.1837 | −23.4865 |
| PM 2 | 1.1258 | 1.7276 | 3.1245 | 16.5672 | 0.4139 | −10.4139 |
| PM 3 | 2.9013 | −0.4895 | −0.4327 | 3.2887 | 1.6074 | −2.6824 |
| PM 4 | 0.5966 | 0.6722 | −0.7214 | 0.3978 | 4.0045 | 0.0553 |

Table V. A comparison of the calculated and simulated values.

| | Elastic deformation of $o$ (mm) | |
|---|---|---|
| | FE model | Analytical result |
| $\delta x$ | −4.12 | −3.8 |
| $\delta y$ | 22.25 | 25.9 |
| $\delta z$ | 2.93 | 2.5 |

model. In the FE model, the spherical joint is replaced by three revolute joints. The linear active leg with prismatic joint is formed using the elastic linear rod. The simulated results based on FE model for the deformation of the terminal platform are solved as shown in Fig. 3.

A comparison of the results based on the FE model and the analytical model for the elastic deformation of $o_4$ for 4(2-UPS/PS+RPS) SHRM is listed in Table V.

The results in Table V shows that the elastic deformation derived from the FE model for 4(2-UPS/PS+RPS) SHRM is basically coincident with the analytical solutions, which is acceptable for stiffness analysis.

## 6. Conclusion

The contribution of this paper lies in the presentation and analysis of a novel n(2-UPS/PS+RPS) SHRM. For kinematics analysis, the forward displacement of the 2-UPS/PS+RPS PM is derived in close form. The result show that one platform of the single PM can reach at most 24 different poses, or mechanical assemblies, with respect to the other platform. This result leads to the 4(2-UPS/PS+RPS) SHRM has $24^4 = 331{,}776$ forward solutions. In addition, compact and elegant expressions for solving the forward velocity of 2-UPS/PS+RPS SHRM are derived. The formulae for solving the statics and stiffness of n(2-UPS/PS+RPS) SHRM are derived. From the statics formula, the active forces and constrained forces in PS and RPS constrained legs are solved respectively. From the stiffness model, the deformations produced by both active and constrained forces in UPS, SP and RPS legs, and the $6\times 6$ stiffness matrix of n(2-UPS/PS+RPS) SHRM are derived completely.

A numerical example, which consists of the kinematics, statics, elastic deformations and stiffness for a 4(2-UPS/PS+RPS) SHRM, is included as a case study. The analytical results are verified by CAD software.

## Acknowledgements

The authors are grateful to the project (No. 51305382) supported by National Natural Science Foundation of China, the financial support of State Key Laboratory of Robotics and System (HIT)

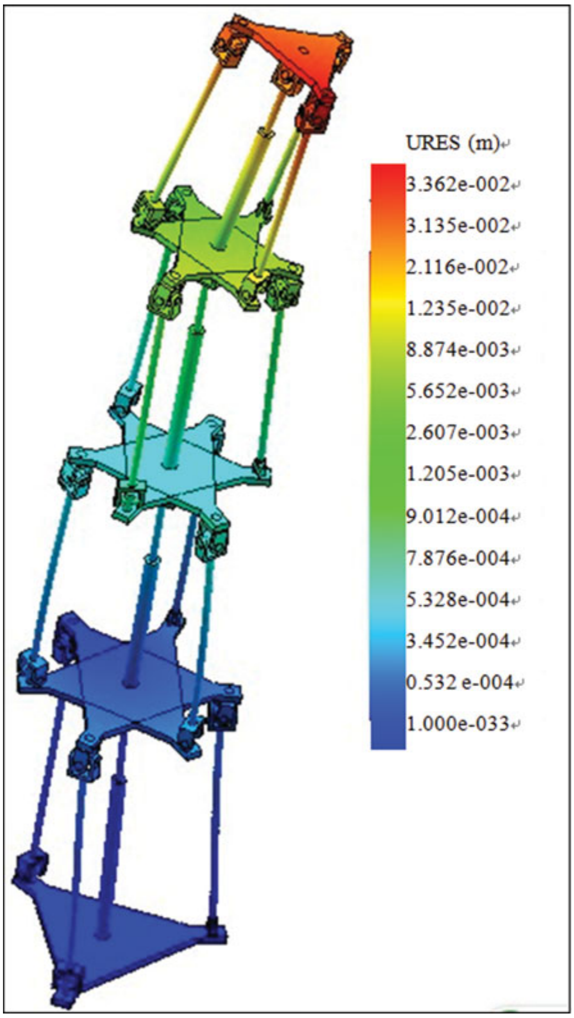


Fig. 3. Simulated result for elastic deformations of a 4(2-UPS/PS+RPS) SHRM.

(No. SKLRS-2012-MS-01), the Key Planned Project of Hebei application Foundation (No. 11962127D) and the Science and Technology Planning Project of Hebei Province (13211610).

## References

1. J.-P. Merlet, *Parallel Robots*, (Kluwer Academic Publishers, London, 2000).
2. J. Angeles, *Fundamentals of Robotic Mechanical Systems*, (Springer-Verlag, Berlin, 2003).
3. M. Shugen and T. Naoki, “Analysis of creeping locomotion of a snake-like robot on a slope,” *Auton. Rob.* **20**(1), 15–23 (2006).
4. M. W. Hanan and I. A. Walker, “Kinematics and the implementation of an elephant’s trunk manipulator and other continuum style robots,” *J. Rob. Syst.* **20**(2), 45–63 (2003).
5. L. Romdhane, “Design and analysis of a hybrid serial-parallel manipulator,” *Mech. Mach. Theory* **34**(7), 1037–1055 (1999).
6. C. Lange, F. Ranjbaran and J. Angeles, “The kinematics of the swashplate mechanism of a vtol unmanned aerial vehicle,” *Multibody Syst. Dyn.* **3**(4), 333–365 (1999).
7. B. Hu, “Formulation of unified Jacobian for serial-parallel manipulators,” *Robot. Comput.-Integr. Manuf.* **30**(5), 460–467 (2014).
8. Y. Lu, B. Hu et al., “Analyses of velocity, acceleration, statics, and workspace of a 2(3-SPR) serial-parallel manipulator,” *Robotica* **27**(4), 529–538 (2009).
9. J. Gallardo and J. Posadas, “Mobility analysis and kinematics of the semi-general 2(3-RPS) series-parallel manipulator,” *Robot. Comput.-Integr. Manuf.* **29**(6), 463–472 (2013).
10. J. Gallardo, R. Lesso, J. Rico et al., “The kinematics of modular spatial hyper-redundant manipulators formed from RPS-type limbs,” *Robot. Auton. Syst.* **59**(1), 12–21 (2011).

11. J. Gallardo, C. R. Aguila et al., “Solving the kinematics and dynamics of a modular spatial hyper-redundant manipulator by means of screw theory,” *Multibody Syst. Dyn.* **20**(4), 307–325 (2008).
12. O. Ibrahim and W. Khalil, “Inverse and direct dynamic models of hybrid robots,” *Mech. Mach. Theory* **45**(4), 627–640 (2010).
13. C. Liang and M. Ceccarelli, “Design and simulation of awaist–trunksystem for ahumanoid robot,” *Mech. Mach. Theory* **53**(7), 50–65 (2012).
14. C. Liang, M. Ceccarelli and G. Carbone, “Experimental characterization of operation of a waist-trunk system with parallel manipulators,” *Chin. J. Mech. Eng.* **24**(5), 713–722 (2011).
15. S. Joshi and L. W. Tsai, “The kinematics of a class of 3-dof, 4-legged parallel manipulators,” *J. Mech. Des.* **125**(1), 52–60 (2003).
16. L. J. Puglisi, R. J. Saltaren et al., “Dimensional synthesis of a spherical parallel manipulator based on the evaluation of global performance indexes,” *Robot. Auton. Syst.* **60**(8), 1037–1045 (2012).
17. G. Cheng, J. Yu and W. Gu, “Kinematic analysis of 3SPS+1PS bionic parallel test platform for hip joint simulator based on unit quaternion,” *Robot. Comput.-Integr. Manuf.* **28**(2), 257–264 (2012).
18. Y. Lu and B. Hu, “Analyzing kinematics and solving active/constrained forces of a 3SPU+ UPR parallel manipulator,” *Mech. Mach. Theory* **42**(10), 1298–1313 (2007).
19. Y. Lu and B. Hu, “Unification and simplification of velocity/acceleration of limited-dof parallel manipulators with linear active legs,” *Mech. Mach. Theory* **43**(9), 1112–1128 (2008).
20. Y. Lu, “Using CAD functionalities for the kinematics analysis of spatial parallel manipulators with 3-, 4-, 5-, 6-linearly driven limbs,” *Mach. Mech. Theory* **39**(1), 41–60 (2004).